Experimental Insights into the Nanostructure of the Cores of Topological Defects in Liquid Crystals

Xiaoguang Wang, Young-Ki Kim, Emre Bukusoglu, Bo Zhang, Daniel S. Miller, and Nicholas L. Abbott

Phys. Rev. Lett. **116**, 147801 — Published 4 April 2016

DOI: 10.1103/PhysRevLett.116.147801

Experimental Insights into the Nanostructure of the Cores of Topological Defects in Liquid Crystals

Xiaoguang Wang, Young-Ki Kim, Emre Bukusoglu, Bo Zhang, Daniel S. Miller, and Nicholas L. Abbott

Department of Chemical and Biological Engineering, University of Wisconsin-Madison, Madison, Wisconsin 53706, USA

The nanoscopic structure of the cores of topological defects in anisotropic condensed matter is an unresolved issue, although a number of theoretical predictions have been reported. In the experimental study reported in this Letter, we template the assembly of amphiphilic molecules from the cores of defects in liquid crystals, and thereby provide the first experimental evidence that the cores of singular defects that appear optically to be points (with strength $m = +1$) are nanometer-sized closed-loop, disclination lines. We also analyze this result in the context of a model that describes the influence of amphiphilic assemblies on the free energy and stability of the defects. Overall, our experimental results and theoretical predictions reveal that the cores of defects with opposite strengths (e.g., $m = +1$ versus $m = -1$) differ in ways that profoundly influence processes of molecular self-assembly.

Understanding the structure of topological defects is important to many branches of physics, including cosmology and condensed matter physics, as the defects play a central role in physical processes such as phase transitions [1,2]. Nematic liquid crystals (LCs), condensed phases that exhibit long range orientational order, are particularly attractive model systems for providing insights into the physics of topological defects as the diversity of topological defects in LCs is large, and one can readily observe and manipulate singular and non-singular defects in LCs such as points (hedgehogs in the bulk, and boojums at a surface), lines (dislocations, disclinations), monopoles, solitons, and domain walls [1-9].

The cores of singular defects in nematic LCs have been proposed to possess significantly lower degrees of orientational order as compared to bulk LCs. The simplest models consider the cores of defects to be isotropic nanophases, although more detailed theories have predicted continuously varying molecular order (including biaxiality) within the core [1]. The size of the core region of a singular LC defect can be estimated as $d_c \sim(K/\Box)^{1/2}$, where K is the elastic constant of the LC and $\Box$ is the free energy density cost of disordering the nematic phase to form the defect core, which leads to the estimate that d_c is typically ~10 nm [1,3,4]. Although topological defects in LCs have been observed to influence interparticle interactions and assemblies [10-17], induce gelation of colloidal dispersions [18,19], and template polymerization in defect-rich phases such as blue phases [20-22], the structure and properties of the cores of defects remains a largely unsolved problem.

Very recently it was reported that the cores of singular line defects (disclinations) of strength $m = -1/2$ can selectively trigger the self-association of amphiphilic molecules into well-defined nanostructures [23]. The signatures of molecular self-assembly, including 'cooperativity', reversibility and controlled growth were observed, with strong analogies to the cooperative co-assembly of amphiphiles and polymers. The measured dependence of the critical association concentration (CAC) on the tail-length of the amphiphiles was consistent with an entropic driving force for self-assembly, derived from the transfer of the flexible tails of the amphiphiles from the ordered bulk LC to the disorder core of the defect. It was also demonstrated that molecular assemblies formed within the LC defects could be preserved by using photo-reactive lipids.

In this Letter, we move beyond the above-described past study of $m = -1/2$ disclinations to report on the self-assembly of lipids within point defects of strength $m = \pm 1$ (formed in a cylindrical capillary, see Fig. 1(a)). The study was motivated by open questions regarding the nanostructure of the cores of $m = \pm 1$ defects. Previous theoretical studies have predicted that point defects with strength $m = \pm 1$ are energetically unstable relative to a nanometer-sized closed-loop disclination of strength $m = \pm 1/2$ (Figs. 2(a)—2(d)) [24-30], although the prediction has yet to be experimentally verified. By characterizing photo-cross-linked assemblies of lipids templated by point defects in capillaries, we report on the interplay of molecular self-assembly and the nanostructure of LC defects, and thereby provide evidence that defects that appear optically to be points of strength $m = +1$ have cores that are in fact nanoscopic disclination loops.

Point defects of strength $m = \pm 1$ were prepared by heating pentylcyanobiphenyl (5CB) into an isotropic phase that was subsequently wicked into capillaries with inner diameters of 400 μm. The inner surfaces of

the capillaries were chemically-functionalized with N,N-dimethyl-N-octadecyl-3-aminopropyl-trimethoxysilyl chloride (DMOAP) to induce perpendicular (homeotropic) anchoring of the LC director $\hat{\mathbf{n}}$ (additional details can be found in the Supplemental Material (SM)). After injection, the 5CB was quenched into the nematic phase. The temperature was subsequently held constant to prevent flow due to

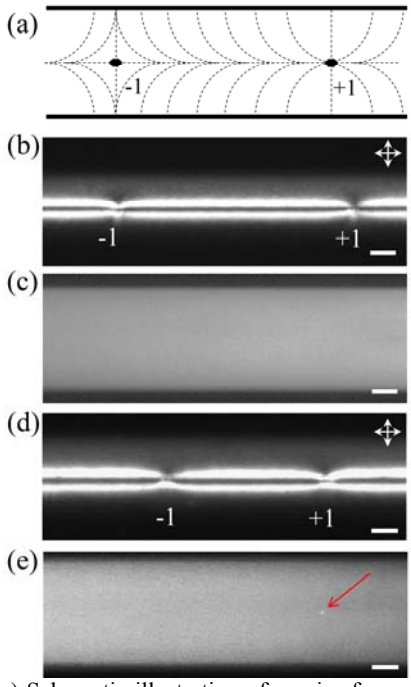

FIG. 1. (a) Schematic illustration of a pair of apparent point defects with strength m = +1 and -1 formed in a capillary filled with nematic LC. The inner surface of the capillary caused perpendicular anchoring of the LC. Dashed line illustrates local ordering of mesogens. (b),(d) Polarized light micrographs of point defects and (c),(e) fluorescence micrographs showing the distribution of amphiphiles (DLPC concentrations are 40 μM in (b),(c) and 47 μM in (d),(e); the DLPC is mixed with BODIPY-C5 at 3% mol/mol based on DLPC). The red arrow in (e) indicates the localization of a molecular assembly of DLPC and BODIPY-C5 at the defect that appears optically to have strength +1. The white double-headed arrows indicate the orientations of crossed polarizers. Scale bars, 100 μm.

thermal-expansion of 5CB [31-33]. In this geometry, $\hat{\mathbf{n}}$ escapes in the direction of the capillary axis, leading to point singularities at domain boundaries [1,3]. Figs. 1(a) and 1(b) show, respectively, a schematic illustration and a representative polarized light micrograph of a pair of m = ±1 point defects (also see SM for optical characterization of the defects). To determine how point defects influence the self-assembly of amphiphiles, we prepared 5CB containing the phospholipid 1,2-dilauroyl-sn-glycero-3-phosphocholine (DLPC) at concentrations ranging from 1.9 to 950 μM. Fluorescence-based detection of DLPC assemblies formed at defects was performed by mixing DLPC with 4,4-difluoro-5,7-dimethyl-4-bora-3a,4a-diaza-*s*-indacene-3-pentanoic acid (BODIPY-C5; 3% mol / mol based on DLPC; see SM for additional details).

For concentrations of DLPC in 5CB up to 40 μM, we measured no significant difference between the intensity of the fluorescence emitted from the point defects and the bulk LC, Fig. 1(c). This result is consistent with a uniform distribution of DLPC between the point defects and the bulk LC. When the concentration of DLPC in 5CB was increased to 47 μM, however, the +1 point defect exhibited a stronger fluorescence signal than the bulk LC, as shown in Fig. 1(e). Interestingly, in contrast, there was no measurable difference between the intensity of fluorescence from the -1 point defect and bulk LC. These results hint that above a threshold concentration (47 μM), DLPC partitions into the nanoenvironment defined by the +1 point defect whereas it remains uniformly dispersed between the bulk LC and -1 point defect. This selective association of DLPC with +1 point defects over -1 defects persisted up to a second threshold concentration (~ 570 μM), above which DLPC aggregates were observed to form in the bulk of the LC and to localize at both ±1 defects (see SM for details). We comment here that the above-described partitioning of amphiphiles to the +1 point defects at concentrations of DLPC between 47 and 570 μM did not lead to optically measurable changes in $\hat{\mathbf{n}}$ in regions of LCs surrounding the defects (consistent with the presence of a nanoscopic assembly of DLPC in the defect core that was smaller than the extrapolation length of the LC). We also note here that, above the first threshold concentration, molecular assemblies were observed within seconds of generation of the LC defects. We did not measure the fluorescence intensities of the assemblies to change over the duration of our observations.

We make three key observations regarding the results above. First, the observation that a threshold concentration of DLPC must be reached to initiate partitioning of DLPC into +1 point defects (i.e., a CAC) is consistent with a cooperative process of molecular self-assembly within the defects. The formation of these assemblies was also measured to be reversible (see SM for details), indicating that they are stabilized thermodynamically (see below for characterization of the nanostructure of the assemblies) [34]. Second, at concentrations of DLPC below 570 μM (see above), association of DLPC occurred in +1 point defects but not in the bulk LC. Furthermore, DLPC assemblies did not form in the non-singular escaped line defect (central region of capillary where $\hat{\mathbf{n}}$ is parallel to capillary axis), confirming that the disordered core of the singular defect is necessary to trigger molecular self-assembly.

Third, we observe that the cores of different types of singular defects differ in their influence on molecular self-assembly of DLPC. Specifically, we calculated the standard free energy change ΔG_1^o ($\Delta G_1^o = k_B T \ln x_{lipid,CAC}$) for the transfer of a DLPC molecule from bulk LC to an assembly formed in a defect core to be -11.4 $k_B T$ for +1 defects and -12.3 $k_B T$ for -1/2 disclinations (CAC ~ 19 μM)[23]. As noted above, for DLPC, we did not observe the cores of -1 defects to template self-assembly prior to the onset of aggregation in the bulk LC. In this case, ΔG_1^o is -8.9 $k_B T$ or smaller (CAC > 570 μM). These observations lead us to conclude that a singular defect is a necessary but not sufficient condition to selectively trigger molecular self-assembly (i.e., before it occurs in bulk LCs). We return to this point below.

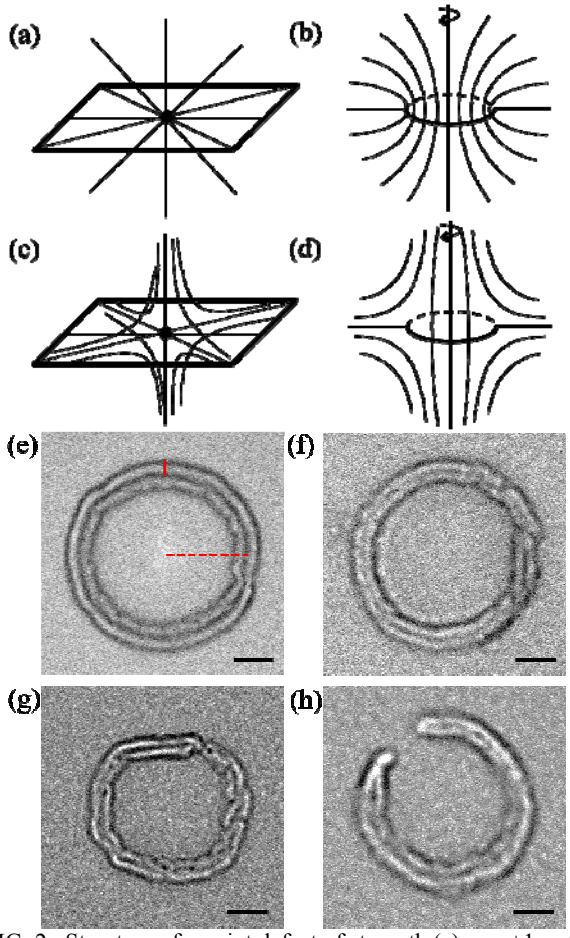

FIG. 2. Structure of a point defect of strength (a) m = +1 or (c) -1 and a disclination loop of strength (b) m = +1/2 or (d) -1/2. (e)—(h) Representative TEM images of amphiphilic molecular assemblies templated by defects that appear optically to be points with strength m = +1. Red solid and dashed lines in (e) indicate the minor and major radii of the toroidal assembly of amphiphiles, respectively. Scale bars, 20 nm.

To crosslink the molecular assemblies formed in +1 defects, we used a photoreactive lipid (diyne-PC doped 3 % BODIPY-C5) instead of DLPC. After UV-crosslinking of the diyne-PC, the assemblies were localized by fluorescence imaging (see SM for details) and then transferred to carbon film-coated grids for further characterization with transmission electron microscopy (TEM). Representative TEM micrographs of the polymeric assemblies are shown in Figs. 2(e)—2(h). Interestingly, toroidal assemblies of lipids, but not globular objects, were observed. The major and minor radii of the toroids shown in Fig. 2 (see Fig. 2(e) for definitions) were measured to be 39 ± 4 nm and 7 ± 1 nm, respectively. We note here that the head-groups of the amphiphiles are electron dense and give rise to the dark regions in the electron micrographs. Inspection of Figs. 2(e)—2(h) reveals three dark regions, which leads us to propose that the toroids are comprised of three periodic lipid bilayers, as shown schematically in Fig. 3.

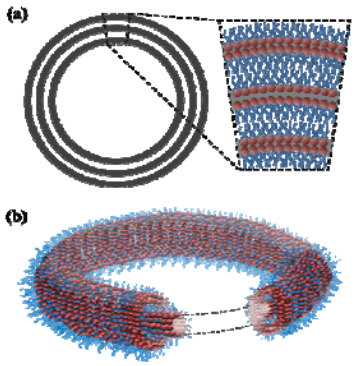

FIG. 3. Schematic illustration of (a) cross-section and (b) toroidal shape of molecular assembly formed within a nanoscopic loop disclination of strength +1/2.

To provide insight into the interplay of molecular self-assembly and defect stability that underlies the above-described experiments, we compared the free energies of m = ±1/2 disclination loops relative to m = ±1 point singularities in the presence and absence of assemblies of lipids. Specifically, we evaluated the free energy F of a defect of strength m decorated with a lipid assembly as

(1)

where F^{defect} is the free energy of formation of the LC defect from a uniformly aligned LC, $F^{association}$ is the standard free energy of formation of the lipid assembly in the defect core, and $F^{demixing}$ is the free energy penalty associated with demixing of lipids in the bulk LC that necessarily accompanies formation of the assembly in the defect core (see SM for details). As detailed elsewhere [1,2,24-26,29,35], we evaluated F^{defect} for the ±1/2 disclination line and ±1 point defect as

$$F_{+1/2}^{defect} = \left\{ 8\pi R\left(K - K_{24}\right) + 2\pi^2 K_{24} a + \frac{\pi^2}{2} Ka\left[\ln\left(\frac{1}{2r_{+1/2}}\right) - 5 \right] \right\}_{\text{elastic}} + \left(2\pi^2 r_{+1/2}^2 a\varepsilon_c\right)_{\text{core}} + \left[4\pi^2 r_{+1/2} a\sigma_o \left(1 + \frac{w}{2}\right) \right]_{\text{surface}} \quad (2)$$

$$F_{-1/2}^{defect} = \left\{ \frac{8}{3}\pi R\left(K + K_{24}\right) + 2\pi a\left(-3.79K + \pi K_{24}\right) + \frac{\pi^2}{2} Ka \ln\left(\frac{1}{2r_{-1/2}}\right) \right\}_{\text{elastic}} + \left(2\pi^2 r_{-1/2}^2 a\varepsilon_c\right)_{\text{core}} + \left[4\pi^2 r_{-1/2} a\sigma_o \left(1 + \frac{w}{2}\right) \right]_{\text{surface}} \quad (3)$$

$$F_{+1}^{defect} = \left[8\pi\left(K - K_{24}\right)\left(R - r_{+1}\right) \right]_{\text{elastic}} + \left(\frac{4}{3}\pi r_{+1}^3 \varepsilon_c\right)_{\text{core}} + \left(4\pi r_{+1}^2 a\sigma_o\right)_{\text{surface}} \quad (4)$$

$$F_{-1}^{defect} = \left[\frac{8}{3}\pi\left(K + K_{24}\right)\left(R - r_{-1}\right) \right]_{\text{elastic}} + \left(\frac{4}{3}\pi r_{-1}^3 \varepsilon_c\right)_{\text{core}} + \left(4\pi r_{-1}^2 a\sigma_o\right)_{\text{surface}} \quad (5)$$

where K is the elastic constant of the nematic LC (for simplicity, assumed to be equal for splay, bend and twist), K_{24} is the saddle-splay elastic constant, R is the size of the system, r_m is the radius of the defect core of strength m, ε_c is the free energy density of the defect core, a is the major radius of the toroid ($a \geq r_{\pm 1/2}$), σ_o is the isotropic—nematic interfacial tension, and w is the surface anchoring energy coefficient. In brief, the first set of terms on the right side of equations (2)-(5) describe the elastic free energy of the LCs outside the core of the defect. The second term represents the excess free energies of the defect cores. The third term is an interfacial energy between the defect core (for simplicity, modeled as an isotropic nanophase) and the surrounding LCs. Details regarding the evaluation of $F^{association}$ and $F^{demixing}$ can be found in SM.

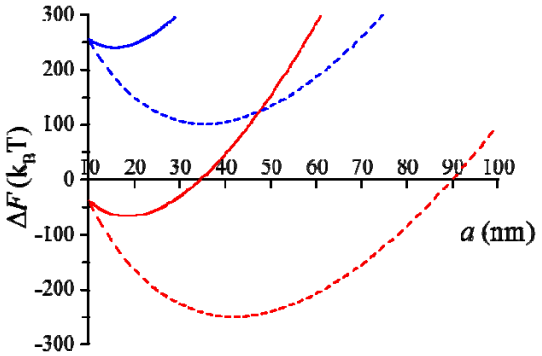

FIG. 4. Difference in free energy ΔF between a disclination loop of strength m = +1/2 (red) or -1/2 (blue) and a point defect of strength m = +1 (red) or -1 (blue) plotted as a function of the radius of the disclination loop a in the absence (solid curve) or presence (dashed curve) of lipid assemblies within the core of the defects.

In Fig. 4, we evaluate the relative free energies of defects of strength ±1/2 and ±1 ($\Delta F = F_{\pm 1/2} - F_{\pm 1}$), both in the presence and absence of lipid assemblies, as a function of a using the following parameters: K = 10 pN, $K_{24} \sim 0.7\ K$ [36,37], $r_{\pm 1/2}$ = 10 nm, $r_{\pm 1} = 1.68\ r_{\pm 1/2}$, $\varepsilon_c = 3\times10^4$ J/m^3, T = 298 K, CAC = 50 μM, $\sigma_0 = 10^{-5}$ J/m^2, and $w = 10^{-2}$ [2] (see SM for details). We make three key comments using Fig. 4. First, the red dashed curve reveals that in the presence of lipid assemblies, a disclination loop of strength +1/2 with an equilibrium radius a_{min} ($(\partial F_{\pm 1/2}/\partial a)|_{a\min}$=0) of 42 nm is predicted to be more stable than a point defect of strength +1. While this calculation supports our experimental observations, we note that the close quantitative agreement between the predicted radius and experimental observation a = 39 ± 4 nm is not significant given the primitive nature of our model. Second, importantly, however, when using the same parameter values that reproduced our experimental observation, we also predict the +1/2 loop disclination to be more stable than the +1 point defect in the absence of a lipid assembly (red solid curve in Fig. 4). In this case, the equilibrium radius a_{min} decreased to ~ 18 nm. Thus, although the favorable thermodynamics associated with formation of the toroidal lipid assembly in the defect core expands the radius of the defect core, we conclude that the +1/2 defect loop is also stable in the absence of the lipid. Third, in contrast to the defects of positive strength, our model predicts the -1 point defect to be stable relative to a -1/2 loop disclination ($\Delta F > 0$), both in the absence and presence of amphiphiles (blue curves in Fig. 4; see detailed discussion in SM) [27,28]. This result is consistent with our above-stated experimental observation of the absence of molecular assemblies within apparent -1 point defects, and hints that the cores of different defects have distinct influences on processes of molecular self-assembly.

Overall, the results above reveal that +1 point defects in LCs template the formation of toroidal lipid assemblies with a major radius of 39 ± 4 nm, consistent with a defect core that is a nanoscopic disclination loop. To the best of our knowledge, this is the first experimental evidence that a circular loop disclination of m = +1/2 is energetically favored against a point singularity of m = +1 in a classical uniaxial LC. We note that the predicted size of the disclination core is too small to be resolved by optical microscopy (the defect appears optically to be a point defect), and direct electron microscopy is challenging due to the weak contrast between the defect and bulk LC. More broadly, the results reported in this Letter demonstrate that molecular self-assembly can be used to provide insights into the nanostructure of topological defects in LCs. Our results also define a number of key questions regarding the nature of the cores of LC defects. For example, our results clearly reveal that the cores of different types of defect differ in local ordering, as reflected in the different CACs of DLPC in +1/2 and -1/2 disclinations, and the absence of selective self-assembly (relative to the bulk LC) in the defects of m = -1. Additional studies are need to elucidate these differences. In addition, our conclusion that the self-

assembly of the lipid influences the sizes of the looped disclinations with strength $m = +1/2$ leads us to predict that the toroidal major radius may provide a sensitive measure of the thermodynamics of amphiphile self-assembly processes. We also anticipate that it will depend on lipid molecular architecture [38,39]. Finally, we comment that we have observed +1 and -1 defects to annihilate each other in the presence of DLPC, although the dynamics are clearly altered by the DLPC assemblies in the defect cores. The influence of molecular assemblies of lipids on defect dynamics has the potential to provide fundamental insights into the roles of defects in phase transitions in soft matter systems.

This work was supported by the National Science Foundation (under awards DMR-1121288 (MRSEC) and CBET-1263970), the Army Research Office (W911-NF-11-1-0251 and W911-NF-14-1-0140), and the National Institutes of Health (AI092004).

[1] M. Kleman and O. D. Lavrentovich, *Soft matter physics: An introduction* (Springer, New York, 2003), Partially Ordered Systems.
[2] Y.-K. Kim, S. V. Shiyanovskii, and O. D. Lavrentovich, J. Phys.: Condens. Matter **25**, 404202 (2013).
[3] P. G. de Gennes and J. Prost, *The physics of liquid crystals* (Clarendon Press, Oxford, 1993).
[4] O. D. Lavrentovich, P. Psini, C. Zannoni, and S. Žumer, *Defects in Liquid Crystals: Computer Simulations, Theory and Experiments* (Springer, Dordrecht, 2001).
[5] M. Kleman and O. D. Lavrentovich, Philos. Mag. **86**, 4117 (2006).
[6] Y.-K. Kim, B. Senyuk, S.-T. Shin, A. Kohlmeier, G. H. Mehl, and O. D. Lavrentovich, Soft Matter **10**, 500 (2014).
[7] C. Zhang, M. Gao, N. Diorio, W. Weissflog, U. Baumeister, S. Sprunt, J. T. Gleeson, and A. Jákli, Phys. Rev. Lett. **109**, 107802 (2012).
[8] Y.-K. Kim, R. Breckon, S. Chakraborty, M. Gao, S. N. Sprunt, J. T. Gleeson, R. J. Twieg, A. Jákli, and O. D. Lavrentovich, Liq. Crysts. **41**, 1345 (2014).
[9] Y.-K. Kim, G. Cukrov, J. Xiang, S.-T. Shin, and O. D. Lavrentovich, Soft Matter **11**, 3963 (2015).
[10] D. Pires, J. B. Fleury, and Y. Galerne, Phys. Rev. Lett. **98**, 247801 (2007).
[11] D. K. Yoon, M. C. Choi, Y. H. Kim, M. W. Kim, O. D. Lavrentovich, and H. T. Jung, Nat. Mater. **6**, 866 (2007).
[12] M. Škarabot, M. Ravnik, S. Žumer, U. Tkalec, I. Poberaj, D. Babič, and I. Musevic, Phys. Rev. E **77**, 061706 (2008).
[13] W. Dickson, G. A. Wurtz, P. R. Evans, R. J. Pollard, and A. V. Zayats, Nano Lett. **8**, 281 (2008).
[14] J. B. Fleury, D. Pires, and Y. Galerne, Phys. Rev. Lett. **103**, 267801 (2009).
[15] Q. Liu, Y. Cui, D. Gardner, X. Li, S. He, and I. I. Smalyukh, Nano Lett. **10**, 1347 (2010).
[16] U. Tkalec, M. Ravnik, S. Čopar, S. Žumer, and I. Muševič, Science **333**, 62 (2011).
[17] D. Coursault, J. Grand, B. Zappone, H. Ayeb, G. Levi, N. Felidj, and E. Lacaze, Adv. Mater. **24**, 1461 (2012).
[18] T. A. Wood, J. S. Lintuvuori, A. B. Schofield, D. Marenduzzo, and W. C. K. Poon, Science **334**, 79 (2011).
[19] E. Bukusoglu, S. K. Pal, J. J. de Pablo, and N. L. Abbott, Soft Matter **10**, 1602 (2014).
[20] H. Kikuchi, M. Yokota, Y. Hisakado, H. Yang, and T. Kajiyama, Nat. Mater. **1**, 64 (2002).
[21] F. Castles *et al.*, Nat. Mater. **11**, 599 (2012).
[22] J. Xiang and O. D. Lavrentovich, Appl. Phys. Lett. **103**, 051112 (2013).
[23] X. Wang, D. S. Miller, E. Bukusoglu, J. J. de Pablo, and N. L. Abbott, Nat. Mater. **15**, 106 (2016).
[24] H. Mori and H. Nakanishi, J. Phys. Soc. Japan **57**, 1281 (1988).
[25] E. M. Terentjev, Phys. Rev. E **51**, 1330 (1995).
[26] O. D. Lavrentovich, T. Ishikawa, and E. M. Terentjev, Mol. Cryst. Liq. Cryst. **299**, 301 (1997).
[27] Z. Bradač, S. Kralj, M. Svetec, and S. Žumer, Phys. Rev. E **67**, 050702 (2003).
[28] G. de Luca and A. D. Rey, J. Chem. Phys. **126** 094907 (2007).
[29] M. Svetec, S. Kralj, Z. Bradač, and S. Žumer, Eur. Phys. J. E **20**, 71 (2006).
[30] V. Tomar, S. I. Hernandez, N. L. Abbott, J. P. Hernandez-Ortiz, and J. J. de Pablo, Soft Matter **8**, 8679 (2012).
[31] Y.-K. Kim *et al.*, Soft Matter **8**, 8880 (2012).
[32] Y.-K. Kim, B. Senyuk, and O. D. Lavrentovich, Nat. Commun. **3**, 1133 (2012).
[33] O. D. Lavrentovich, Y.-K. Kim, and B. I. Senyuk, Proc. of SPIE **OP211**, 84750G 1 (2012).
[34] P. S. Hiemenz and R. Rajagopalan, *Principles of Colloidal and Surface Chemistry* (CRC, London, 1997).
[35] J.-I. Fukuda and H. Yokoyama, Phys. Rev. E. **66**, 012703 (2002).
[36] O. D. Lavrentovich and V. M. Pergamenshchik, Phys. Rev. Lett. **73**, 979 (1994).
[37] H. Stark, Phys. Rep. **351**, 387 (2001).
[38] I. H. Lin, D. S. Miller, P. J. Bertics, C. J. Murphy, J. J. de Pablo, and N. L. Abbott, Science **332**, 1297 (2011).
[39] D. S. Miller and N. L. Abbott, Soft Matter **9**, 374 (2013).